Emission characteristics and dynamics of C_2 from laser produced graphite plasma

S. S. Harilal, Riju C. Issac, C. V. Bindhu, V. P. N. Nampoori, and C. P. G. Vallabhan[a)]
Laser Division, International School of Photonics, Cochin University of Science & Technology, Cochin 682 022, India

(Received 2 December 1996; accepted for publication 20 December 1996)

The emission features of laser ablated graphite plume generated in a helium ambient atmosphere have been investigated with time and space resolved plasma diagnostic technique. Time resolved optical emission spectroscopy is employed to reveal the velocity distribution of different species ejected during ablation. At lower values of laser fluences only a slowly propagating component of C_2 is seen. At high fluences emission from C_2 shows a twin peak distribution in time. The formation of an emission peak with diminished time delay giving an energetic peak at higher laser fluences is attributed to many body recombination. It is also observed that these double peaks get modified into triple peak time of flight distribution at distances greater than 16 mm from the target. The occurrence of multiple peaks in the C_2 emission is mainly due to the delays caused from the different formation mechanism of C_2 species. The velocity distribution of the faster peak exhibits an oscillating character with distance from the target surface. [S0021-8979(97)04907-4]

I. INTRODUCTION

Pulsed laser ablation of graphite has become well established as a reliable method for preparation of newly found materials like fullerenes[1–4] and diamond like carbon (DLC) films.[5–12] However, the underlying physics and chemistry of the processes such as carbon cluster formation or their dissociation are less than well understood. Further, the details of the dynamics of laser interaction with materials are extremely important in the context of optimizing the conditions for depositing good quality thin films. It has been shown that high quality DLC films are obtained at low laser fluences where the molecular C_2 emission is most dominant.[13] The relative population of the carbon clusters produced in the laser ablation of graphite has been found to depend on different experimental parameters like laser fluence, nature of background gas and its pressure, relative position of the plasma volume with respect to target surface etc.

Based on the widely accepted theory of the pulsed laser evaporation,[14,15] the physical model of the laser ablation can be explained as follows. In the initial stage, the interaction of the laser beam with the bulk target results in the evaporation of the surface layer. Following this, the interaction of the laser beam with evaporating material leads to the formation of isothermally expanding plasma and this persists until the termination of the laser pulse. In the final stage, adiabatic expansion of the plasma in the forward direction takes place when the target is irradiated under vacuum. The characteristics of the laser plasma strongly depend on the parameters like laser wavelength,[16,17] ambient gas pressure,[18,19] laser energy density[20,21] etc. Several spectroscopic studies of graphite plasma have been carried out[22] using a variety of laser wavelengths such as 193, 248, 308, 532 and 1064 nm. It has been shown that shorter wavelengths are more effective for penetration into the sample, mainly because of large ablation rates possible at these wavelengths.[23] However, the main advantage in the use of near infrared low energy photons is that, they are less likely to invoke photochemistry into the ablation phenomenon.

For the characterization of the photofragmented species in a plasma, many spectroscopic tools are used including emission spectroscopy,[24] laser induced fluorescence,[25] absorption spectroscopy,[26] mass spectroscopy,[27] ion probe method,[28] Michelson interferometry[29] etc. Of these the nonrestrictive methods to study the laser plasmas are mass spectrometry and optical emission spectrometry. Optical emission spectroscopic technique is concerned with the light emitted by electronically excited species in laser induced plasma produced in front of the target surface. Also optical emission measurements are useful for species identification and *in situ* monitoring during deposition. Useful information about the elemental composition of the target material can be obtained from the analysis of the emissions emanating from the plasma plume. The carbon clusters like C_{60} and higher fullerenes are well known to be formed as a product of the laser ablation of graphite in an ambient helium atmosphere. Carbon molecules are particularly interesting due to their unique and fascinating structural and spectroscopic properties, their importance in astrophysical processes and due to their role in combustion and soot formation. Laser ablation has the unique advantage that most of these molecules are formed in their excited states and hence spectroscopic measurements offer an excellent means to investigate their evolution and dynamics.

In this article we report a comprehensive study of spatial characteristic emission from C_2 using time resolved spectroscopy. In these experiments time resolved spectroscopic observations of the plasma plume from graphite under helium ambient atmosphere were carried out to determine the velocities of the ablated C_2 species. Such temporally and spatially resolved high resolution spectroscopic studies are helpful to optimize parameters of DLC film deposition and to

a)Electronic mail: root@cochin.ernet.in

correlate the carbon clusters with plasma dynamics. To the best of our knowledge this is the first report regarding the existence of a triple peak in the temporal history of C_2 emission from laser produced carbon plasma. Our results also indicate that the temporal profile of C_2 species produced during laser ablation of graphite exhibits a triple peak structure only beyond a certain spatial separation from the target (16 mm) and thereafter they propagate with three different expansion velocities.

II. EXPERIMENTAL SETUP

The experimental setup used for the present study is similar to the one described elsewhere.[30,31] The 1.06 μm laser beam from a *Q*-switched Nd:YAG laser having pulse width of 9 ns and repetition rate 10 Hz was focused onto a graphite target contained in a vacuum chamber. The target was rotated by a small electric motor so that the laser pulses are made to fall at a new spot every time on the graphite surface. The pressure of helium gas inside the chamber is kept at 100 mTorr during these experimental studies. The emission from the carbon plasma was focused at right angles to its expansion direction to produce a 1:1 image on the entrance slit of a scanning monochromator (1 m Spex) coupled to a photomultiplier tube (PMT, Thorn EMI, rise time 2 ns). Using a number of apertures and slits emission features from various vertical segments of the plasma plume can be studied. The characteristic emission lines were selected using the monochromator and the output from the PMT was monitored using a digital storage oscilloscope (Iwatsu model DS 8621) with a maximum sampling rate of 200 MHz with 50 Ω termination to record the emission pulse shapes. This setup essentially provides delay as well as decay times for emission from constituent species from vertical segments situated at different distances from the target. In these experiments spatially resolved studies were carried out for distance up to 25 mm normal to the target surface with an accuracy better than 0.2 mm.

III. RESULTS AND DISCUSSION

The time resolved studies of emission lines from C_2 species were made from the oscilloscope traces which showed definite time delays for emission with respect to the laser pulse. It has been found that each emission line has a distinctly different temporal profile. The time evolution of emission from the constituent species of the plasma determines the subsequent expansion and should provide the best observations for shaping our understanding of the plasma dynamics. Time of flight (TOF) distributions give the time of arrival at a certain point in space with a known flight length and these can easily be transformed into velocity distribution.

Recently we reported[30] space as well as time resolved studies of C_2 species which reveal double peak structure in TOF emission pattern of C_2 species beyond a threshold laser fluence. This threshold was found to increase with increasing distance from the target surface. Below this threshold fluence, only single peak distribution is observed. These twin peak structures of C_2 species from carbon plasma beyond a threshold fluence were assigned due to the occurrence of species corresponding to those generated by the dissociation of higher clusters, giving rise to the slower velocity component and to those generated by two body or many body recombination processes giving rise to the faster peak which is present only at higher fluences. It is also observed that the faster peak keeps getting narrow and shifts towards the leading edge of the distribution while the slower one becomes more and more wide and moves away from the leading edge with the increase in helium ambient pressure.[18] The most important results of the present observations is that the temporal profile of C_2 species exhibits a triple peak structure for the TOF distribution at spatial distances greater than 16 mm from the target.

The typical temporal profiles for emission from C_2 species [choosing $\lambda = 516.5$ nm corresponding to (0,0) band of Swan system] at a laser fluence of 29.3 J cm^{-2} for different axial distances from the target are shown in Figs. 1(a)–1(f). The Swan bands arise from transitions between the $a^3\Pi_u$ and $d^3\Pi_g$ electronic states of the molecule. The time resolved observation presented here characterizes the axial expansion of the plasma i.e., strictly along a direction perpendicular to the target surface. Figures 1(a) and (b) represent the oscilloscope traces of TOF distribution of C_2 molecules at distances 5 mm and 10 mm from the target. At these distances, there exits a double peak and the features of these twin peaks on laser fluence and ambient helium pressure have been reported recently.[18,30] The emergence of the new peak occurs only at distances greater than 16 mm from the target. Fig. 1(c) shows the formation of the new peak in between the aforesaid twin peaks. Figures 1(d)–1(f) show the triple fold TOF distribution of the C_2 species at distances 18 mm, 20 mm and 22 mm away from the target. The time evolution of the spectral emission obtained in the present work clearly reveals that the C_2 species ejected from graphite target has a twin peak distribution up to a certain distance from the target (16 mm) and at farther distances the TOF pattern shows a triple peak structure. It has also been found that there is a well defined threshold fluence to observe this triple peak structure in the TOF distribution.

There are only a few reports which describe the multiple peak time of flight distribution in laser generated plasma from graphite target. Dixon and Seely[32] observed a double peak structure in C II species and they explain it as due to collisional interaction like resonance charge transfer which has been shown to be a velocity dependent one. Lowndes[6] observed three modes of incident species in the TOF profile using ion probe method and they attributed it to scattered ions, ions that are slowed by gas phase collisions and slow moving clusters formed through collisions, respectively. Tasaka *et al.*[33] observed triplefold plume structure during Nd:YAG laser ablation of graphite into helium ambient atmosphere and during optical emission studies they found that the fastest component is composed of carbon ions, second fastest component is due to compressed neutral molecules and the slowest component is the radial vapor from the graphite target. Bulgakov and Bulgakova[34] made a theoretical model for the plume expansion into ambient gas and have shown that pulsating character in the velocity distribution

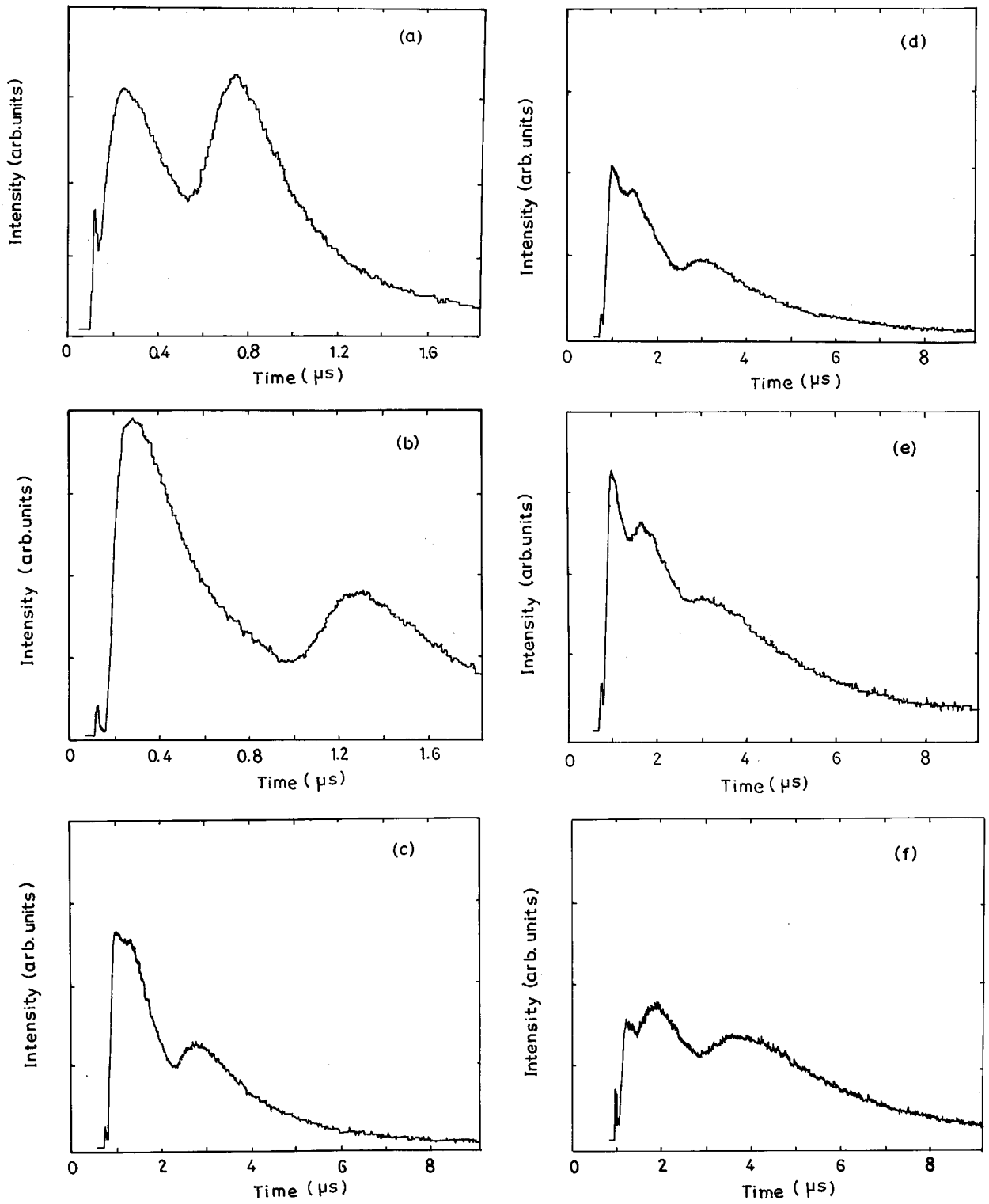

FIG. 1. Intensity variation of spectral emission with time for C_2 species (516.5 nm) at different distances from the target. Distances are (a) 5 mm, (b) 10 mm, (c) 17 mm, (d) 18 mm, (e) 20 mm and (f) 22 mm. These TOF spectra are recorded at a laser fluence of 29.3 J cm^{-2} and at helium pressure of 100 m Torr.

can be explained using back and forth shock wave propagation and they also indicated that ionization and recombination processes have no significant effect on these pulsations. But they couldn't succeed in explaining the triple structure for the BaO molecule during mass spectroscopic studies[35] using cloud ionization model.

It is well known that graphite exhibits a large difference between the inter-layer and the intra-layer bond strengths. It is expected that at low laser fluences, graphite will be ablated layer by layer producing large particles which in turn get dissociated to form C_2 species.[36] The dissociative mechanism can further be supported by the observation of long duration

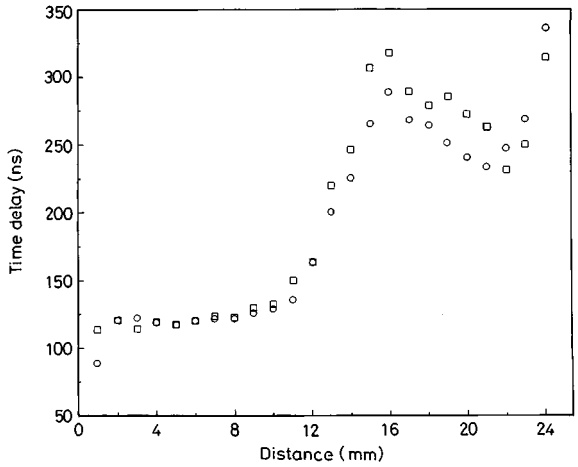

FIG. 2. Variation of time delay in the peak intensities with distance for the Pk1 of C_2 at different laser fluences. (○) 29.3 J cm^{-2} and (□) 31.6 J cm^{-2}.

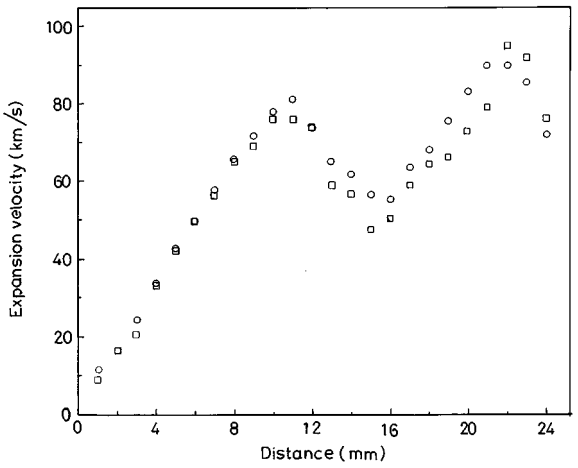

FIG. 4. Expansion velocities as function of distance for Pk1 of C_2 for fluences at (○) 29.3 J cm^{-2} and (□) 31.6 J cm^{-2}.

of Swan band emission at low fluences. At low laser fluences only a slowly propagating component with low kinetic energy is observed. The dominant mechanism for the production of C_2 Swan band emission at low fluences is the electron collision with C_n cations and neutrals ($n>2$) followed by dissociation where one of the fragments is an ejected C_2 molecule. However, at high laser fluence Swan band formation is mainly due to electron–ion and ion–ion recombination.[37] It is observed here that at high laser fluences, after a threshold, an emission peak showing a faster component with higher kinetic energy for C_2 molecules begins to appear.

Figures 2 and 3 give the variation of time delay with distance for the faster ($Pk1$) and slower peak ($Pk2$) in the TOF distribution of C_2 for different laser fluences. It is seen from Fig. 2 that the time delay for the faster peak is constant up to 10 mm from the target and then increases. It is also noted that after 16 mm the delays for the $Pk1$ decreases sharply. From the plots of delay time vs distance, one can obtain instantaneous velocities for C_2 molecules from $Pk1$ and $Pk2$ and these are given in Figures 4 and 5, respectively. It may be noted that the velocities are not constant and they vary with distance from the target. From the mean velocity distribution of these species it is clear that the velocity of $Pk1$ increases with spatial separation from the target up to $z=10$ mm. The sudden decrease in the velocity of these species after 10 mm shows the deceleration of the C_2 species. However at distances greater than $z=15$ mm, the velocity of the particles again gets enhanced. In the case of the second peak (Fig. 5) the velocity increases with spatial separation from the target until it reaches 6 mm and then the expansion velocity is found to be somewhat constant (8 km/s) up to $z=20$ mm and then decreases. The intensity variation of these peaks with spatial separation shows different spatial maxima for faster ($z=12$ mm) and delayed peak (5 mm). The variation of time delay for newly generated peak beyond $z=16$ mm is given in Fig. 6 from which it is clear that the time delay is increasing with increasing distance in this case.

In order to identify whether the multiply ionized carbon species have any role in this peculiar appearance of three peaks in the C_2 emission spectrum, optical emission analysis from carbon ions were also carried out. Emission originating

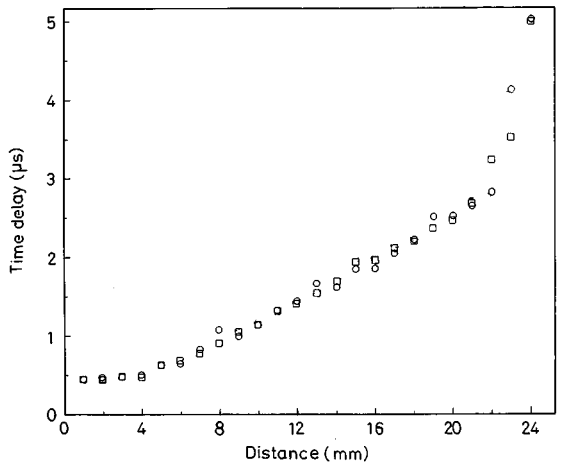

FIG. 3. Variation of time delay in the peak intensities with distance for Pk2 of C_2 at different laser fluences. (○) 29.3 J cm^{-2} and (□) 31.6 J cm^{-2}.

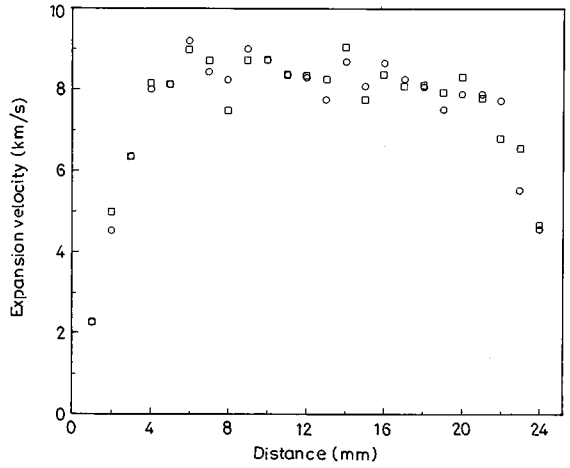

FIG. 5. Expansion velocities as a function of distance for pk 2 of C_2 for fluences at (○) 29.3 J cm^{-2} and (□) 31.6 J cm^{-2}.

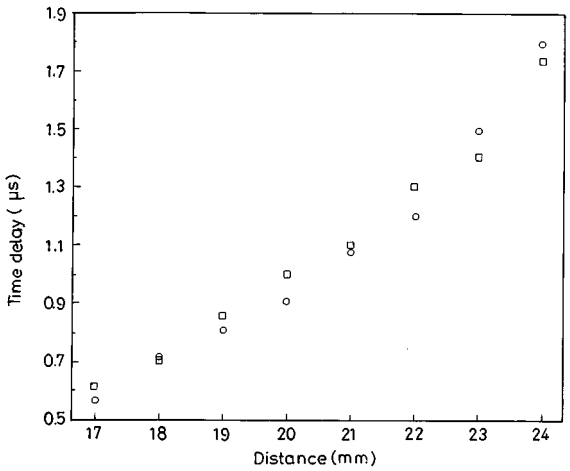

FIG. 6. Variation of delay time with distance for newly generated peak of C_2 at different laser fluences. (○) 29.3 J cm^{-2} and (□) 31.6 J cm^{-2}.

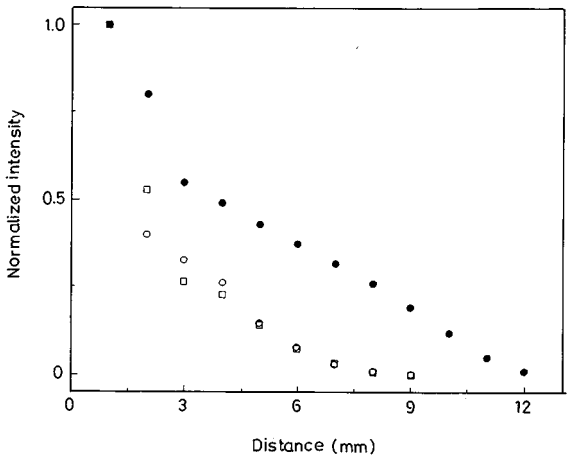

FIG. 8. Change in intensity with distance for different ionic species of carbon. (●) C II transition ($3d^2D-4f^2F^0$) at 426.7 nm, (□) C III transition ($3p^1P^0-3d^1D$) at 580.1 nm and (○) C IV transition ($3s^2S-3p^2P^0$) at 569.5 nm.

from ionic species appears when the laser fluence is sufficient to create a predominantly ionized plasma medium. Temporal profiles are recorded for the ionized carbon species, at 426.7 nm of C II ($3d^2D-4f^2F^0$), 569.5 nm of C III ($3p^1P^0-3d^1D$) and 580.1 nm of C IV ($3s^2S-3p^2P^0$) for different distances from the target. The ionic species are characterized by faster and narrower TOF distribution in comparison with atomic or molecular species. The time delays observed for different ionized species with respect to the axial distance from the target is given in Fig. 7 at a laser fluence of 25.5 J cm^{-2}. The inverse slope of the curve drawn through the points gives their instantaneous velocities of these ionized species at a given time and distance. The expansion velocities of the ionized species are found to be increasing with degree of ionization. It is noted that the maximum expansion velocities of C II, C III and C IV are found to be at 40 km/s, 58 km/s and 80 km/s, respectively. The maximum spatial range for the ions were limited by the exponential drop in recorded intensity with distance (Fig. 8) and the time.

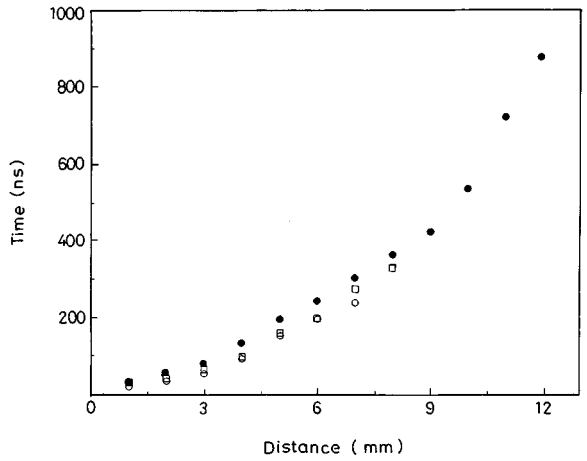

FIG. 7. Variation of time delay in peak intensity with distance for different ionic species of carbon at a laser fluence of 25.5 J cm^{-2}. (●) C II transition ($3d^2D-4f^2F^0$) at 426.7 nm, (□) C III transition ($3p^1P^0-3d^{-1}D$) at 580.1 nm and (○) C IV transition ($3s^2S-3p^2P^0$) at 569.5 nm.

If it is assumed that the terminal stage of the plume can be modeled as a free expansion into the vacuum, the expansion velocity v can be written as[38,39]

$$v=\sqrt{\frac{2\eta kT}{M}}, \tag{1}$$

where M is the mass of the species, η is the number of internal degrees of freedom which varies from 2.53 to 3.28 associated with ionization and excitation, T is the temperature of the plasma and k is the Boltzmann constant. The above equation shows that the time delay of the plasma species depends upon the temperature and dimensions of the plasma along with mass of the concerned species. According to Eq. (1), due to identical masses, different ionic species of carbon should have identical time delays. However, in actual practice it is observed that the species with higher degree of ionization have higher velocities because of the coulomb fields generated by negatively charged electrons escaping from the plume. These results are consistent with our earlier observations[30] suggesting that the occurrence of faster peak in the temporal profile of C_2 above a certain threshold laser fluence is caused by recombination of these ions. It is also supported by the fact that the molecules giving rise to these recombination peaks have almost identical kinetic energy distribution in comparison with highly energetic ions.

Another important observation is that the intensity of the ionized species increases with laser fluences but get saturated at higher fluences as is given in Fig. 9. There is a laser fluence threshold for the appearance of multiply charged ions and this threshold increases with degree of ionization. It is also noted that the expansion velocities of these ionic species increases with increasing laser fluence. The exponential increase in the intensity of emission of positive ions with laser fluence is in accordance with the Richardson–Saha laws.[40] The saturation in intensity at high laser fluences is due to a change in the efficiency of laser coupling to the target by

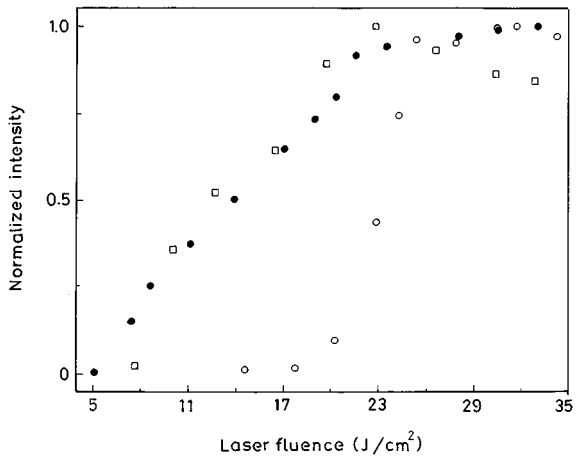

FIG. 9. Change in intensity with laser fluence for different ionic species. (●) C II transition ($3d^2D-4f^2F^0$) at 426.7 nm, (□) C III transition ($3p^1P^0-3d^1D$) at 580.1 nm and (○) C IV transition ($3s^2S-3p^2P^0$) at 569.5 nm.

increased absorption and/or reflection from the laser induced plasma, a process known as plasma shielding. The increase in ionization and intensity saturation with varying laser fluence also seem to suggest strong interaction of the laser pulse with the dense plasma formed near the target within the pulse duration.

From Fig. 1, it is seen that at higher spatial distance from the target (>16 mm), the recombinational peak splits further into two forming a threefold time of flight profile for the C_2 species. The reason for the occurrence of twin peak structure in the recombination emission intensity profile can be attributed to delays caused by different recombinational formation mechanism of C_2 species in the plasma. It is also seen from Fig. 6 that the time delays for these newly generated C_2 species are increasing steadily with increasing distance from the target.

From Fig. 4, one sees an anomalous variation of expansion velocity of the C_2 species with axial separation from the target. Gas dynamic effects are thought to play a major role in determining the spatial and velocity distribution of the vaporized material. The velocity at any point inside the plasma depends upon the spatial separation from the target surface. The atoms, molecules and ions undergo collisions in the high density region near the target forming the so called Knudsen layer, to create a highly directional expansion perpendicular to the target.[41,42] The density of the plasma will be maximum near the target due to collisions and hence the mean drift velocity normal to surface will be a minimum at very close to the target. The plasma expansion in a direction perpendicular to the target surface can be written as[14]

$$Z(t)\left[\frac{1}{2t}\frac{dZ}{dt}+\frac{d^2Z}{dt^2}\right]=\frac{6kT_0}{M}, \tag{2}$$

where dZ/dt is the expansion velocity of the plasma in the Z direction, k, the Boltzmann constant, T_0 the isothermal temperature of the plasma and M is the molecular weight of the particle. The above equation evidently shows that the expansion velocities are low and acceleration is very high during the initial stages of expansion. But when the expansion velocities increase, acceleration starts to decrease. The laser pulse being short, the plasma cloud within the pulse duration has a minimum size in the direction normal to the target surface. A dense plasma can absorb strongly the trailing part of the laser pulse. Thus the absorption of the laser radiation by the plasma increases the velocity of the species inside the plasma and the hydrodynamic expansion is directed right angles to the surface of the target. This is found to be true as seen in Figures 4 and 5, respectively, at distances near the target where expansion velocities increase very rapidly with respect to the spatial separation from the target. During the initial stages of the plasma expansion, the velocity in the direction perpendicular to the target surface is very high as a result of the small dimension of the plasma in that direction. It is reported that[43,44] during shorter time intervals that the expansion of the plume is one dimensional while for longer time scales the expansion is essentially three dimensional. This has also been supported by ultra fast photography of laser ablation plumes.[45]

After the termination of the laser pulse, adiabatic expansion of the plasma begins. During this process, the thermal energy is converted to kinetic energy with the plasma attaining high expansion velocities. The adiabatic expansion of the plasma in the Z direction can be written as[14]

$$Z(t)\left[\frac{d^2Z}{dt^2}\right]=\frac{6kT_0}{M}\left[\frac{Z_0}{Z(t)}\right]^{\gamma-1}, \tag{3}$$

where Z_0 is the edge of the plasma at which the laser pulse is terminated and γ, the maximum attainable particle velocity. In the adiabatic expansion region, the acceleration depends on the initial temperature and the mass of the species.

From Fig. 5 it is seen that, the velocity of Pk2 is constant (8 km/s) after the initial expansion of the plasma. The velocities of these are found to be decreased at the boundary of the plasma which is in accordance with the drag model[46] which predicts that the plume eventually comes to rest due to resistance from collision with background gas. Fig. 4 shows that between distances of 10 mm to 15 mm from the target, the expansion velocity decreases for the Pk1 while it increases again at farther distances. This peculiar velocity pulsations can be explained as follows. During the adiabatic expansion the thermal energy is rapidly converted into kinetic energy, thereby attaining high expansion velocities. It has been reported that for spherical plasmas temperature drops off as the square of its radius.[47] A rapid drop in temperature occurs when the spherical plasmas expand. This may be the reason for the decrease in kinetic energy for the Pk1 in the region between 10 mm to 15 mm. However, the temperature drop will not continue with respect to the square of the radius of the spherical plasmas indefinitely, because of cooling due to expansion which will be balanced by the energy gained from the recombination processes of the ions.

IV. CONCLUSIONS

Time and space resolved study of C_2 molecules from laser produced carbon plasma in the presence of ambient helium gas is carried out using optical emission spectros-

copy. 1.06 μm radiation from a Q-switched Nd:YAG laser was focused onto the graphite target where it produced a transient and elongated plasma. Measurements of spatial dependence of the TOF emission intensities are made up to 25 mm away from the target. An oscillatory behavior is observed in the TOF distribution of C_2 species and this is observed only above a threshold laser fluence. At distances greater than 16 mm from the target, a threefold TOF distribution is observed and the reason for the formation for these peaks is discussed. The peak due to low kinetic energy component, which is observed at all fluences, is formed as a result of dissociation of higher clusters. The departure of single peak velocity distribution at higher laser fluences is due to processes like recombination of the high energetic particles. The energy released on recombination is converted into kinetic energy of the molecules, atoms and ions, which may give rise to a group of relatively faster C_2 species. At farther distances from the target ($>$16 mm) the recombinational peak becomes modified into two due to inherent delays caused by different recombination and excitation mechanisms. It is also found that these results are consistent with kinetic energy distribution of ionic species. The different expansion dynamics of C_2 species in the ambient gas are also discussed. The velocity pulsations in the faster peak during expansion into ambient gas are attributed to nonequilibrium kinetic energy transfer because of many body recombination.

ACKNOWLEDGMENTS

The present work is supported by the Department of Science and Technology, Government of India. One of the authors (SSH) is grateful to Council of Scientific and Industrial Research, New Delhi for a senior research fellowship. RCI and CVB are thankful to University Grants Commission, New Delhi for their research fellowships.

[1] H. W. Kroto, R. J. Heath, S. C. O'Brien, R. F. Curl, and R. E. Smalley, Nature **318**, 165 (1985).
[2] E. A. Rohlfing, J. Chem. Phys. **93**, 7851 (1990).
[3] G. Meijer and D. S. Bethane, J. Phys. Chem. **93**, 7800 (1990).
[4] R. E. Smalley, Acc. Chem. Res. **25**, 98 (1992).
[5] Pulsed laser deposition of thin films, edited by D. B. Chrisey and G. K. Hubler (Wiley, New York, 1994).
[6] D. H. Lowndes, D. B. Geohegan, A. A. Puretzky, D. P. Norton, and C. M. Rouleau, Science **273**, 898 (1996).
[7] D. R. Mckenzie, D. Muller, and B. A. Palithorpe, Phys. Rev. Lett. **67**, 773 (1991).
[8] M. E. Kozlov, K. Yaze, N. Minami, P. Fons, H. A. Durand, A. N. Obraztsov, K. Nozaki, and M. Tokumoto, J. Phys. D **29**, 929 (1996).
[9] D. L. Pappas, K. L. Saenger, J. Bruley, W. Krakow, J. J. Cuomo, T. Gu, and R. W. Collins, J. Appl. Phys. **71**, 5675 (1992).
[10] F. Davanloo, E. M. Juengerman, D. R. Jander, T. J. Lee, and C. B. Collins, J. Appl. Phys. **67**, 2081 (1990).
[11] S. S. Wagal, E. M. Juengerman, and C. B. Collins, Appl. Phys. Lett. **53**, 187 (1988).
[12] G. Dollinger, C. M. Frey, and P. Maier-Komor, Nucl. Instrum. Methods Phys. Res. A **334**, 167 (1993).
[13] Abhilasha and R. K. Thareja, Phys. Lett. A **184**, 99 (1993).
[14] R. K. Singh and J. Narayan, Phys. Rev. B **41**, 8843 (1990).
[15] R. K. Singh, O. W. Holland, and J. Narayan, J. Appl. Phys. **68**, 233 (1990).
[16] J. T. Mckinley, A. Ueda, R. G. Albridge, A. V. Barnes, and Tolk, in Ref. 22, p. 70.
[17] Abhilasha, R. K. Dwivedi, and R. K. Thareja, J. Appl. Phys. **75**, 8237 (1994).
[18] S. S. Harilal, R. C. Issac, C. V. Bindhu, V. P. N. Nampoori, and C. P. G. Vallabhan, Jpn. J. Appl. Phys. (in press).
[19] C. Boulmer-Leborgne, J. Hermann, and B. Dubreulil, Polym. Sci. Technol. **2**, 219 (1993).
[20] S. S. Harilal, P. Radhakrishnan, V. P. N. Nampoori, and C. P. G. Vallabhan, Appl. Phys. Lett. **64**, 3377 (1994).
[21] J. Gonzalo, C. N. Afonso, and J. Perriere, J. Appl. Phys. **79**, 8042 (1996).
[22] P. T. Murray and D. T. Peeler, in *Laser Ablation: Mechanisms and Applications II* (American Institute of Physics, New York, 1994), p. 359.
[23] F. Amiranoff, R. Fabbro, E. Fabre, C. Garban, J. Virmont, and M. Weinfeld, Phys. Rev. Lett. **43**, 522 (1979).
[24] G. Padmaja, A. V. Ravi Kumar, V. P. N. Nampoori, and C. P. G. Vallabhan, J. Phys. D **26**, 35 (1993).
[25] Y. Nakata, W. K. A. Kumuduni, T. Okada, and M. Maeda, Appl. Phys. Lett. **66**, 3206 (1995).
[26] H. F. Sakeek, T. Morrow, W. G. Graham, and O. G. Walmsley, Appl. Phys. Lett. **59**, 3631 (1991).
[27] B. Weinkauf, P. Aicher, G. Wesley, J. Grotemeyer, and E. W. Schlag, J. Chem. Phys. **98**, 8381 (1994).
[28] D. B. Geohegan and A. A. Puretzky, Appl. Phys. Lett. **67**, 197 (1995).
[29] G. K. Varier, S. S. Harilal, C. V. Bindhu, R. C. Issac, V. P. N. Nampoori, and C. P. G. Vallabhan, Spectrochim. Acta B (in press).
[30] S. S. Harilal, R. C. Issac, C. V. Bindhu, V. P. N. Nampoori, and C. P. G. Vallabhan, J. Appl. Phys. **80**, 3561 (1996).
[31] S. S. Harilal, R. C. Issac, C. V. Bindhu, V. P. N. Nampoori, and C. P. G. Vallabhan, Pramana, J. Phys. **46**, 145 (1996).
[32] R. H. Dixon and R. C. Elton, Phys. Rev. Lett. **38**, 1072 (1977).
[33] Y. Tasaka, M. Tanaka, and S. Usami, Jpn. J. Appl. Phys. 1 **34**, 1673 (1995).
[34] A. V. Bulgakov and N. M. Bulgakova, J. Phys. D **28**, 1710 (1995).
[35] W. K. A. Kumuduni, Y. Nakayama, Y. Nakata, T. Okada, and M. Maeda, J. Appl. Phys. **74**, 7510 (1993).
[36] Y. Iida and E. S. Yeung, Appl. Spectrosc. **48**, 945 (1994).
[37] D. L. Pappas, K. L. Saenger, J. J. Cuomo, and R. N. Dreyfus, J. Appl. Phys. **72**, 3966 (1992).
[38] R. W. Dreyfus, R. Kelly, and R. E. Walkup, Nucl. Instrum. Methods Phys. Res. B **23**, 557 (1987).
[39] R. Kelly and A. Miotello, in *Pulsed Laser Deposition of Thin Films*, edited by D. B. Chrisey and G. K. Hubler (Wiley, New York, 1994), Chap. 3.
[40] E. N. Sobol, in *Phase Transformation and Ablation in Laser Treated Solids* (Wiley, New York, 1994), Ch. 6.
[41] R. Kelly and R. W. Dreyfus, Surf. Sci. **198**, 263 (1988).
[42] R. Kelly, Phys. Rev. A **46**, 860 (1992).
[43] W. Pietsch, B. Dubreuil, and A. Briand, Appl. Phys. B **61**, 267 (1995).
[44] J. C. S. Kools, T. S. Baller, S. T. Dezwart, and J. Dielemen, J. Appl. Phys. **71**, 4547 (1992).
[45] A. Gupta, B. Baren, K. G. Casey, B. W. Husley, and R. Kelly, Appl. Phys. Lett. **59**, 1302 (1991).
[46] D. B. Geohegan, Thin Solid Films **220**, 138 (1992).
[47] J. M. Dawson, Phys. Fluids **7**, 981 (1964).